Computer Modeling in
Engineering & Sciences

Tech Science Press

https://doi.org/10.32604/cmes.2026.086869

ARTICLE

Deep Learning-Based Spatiotemporal Surrogate Framework for Reconstructing Transient 3D Hydrogen Explosion Overpressure Fields

Jiwon Hwang and Sangjun Lee*

Department of AI and SW Convergence, Soongsil University, Seoul, Republic of Korea

*Corresponding Author: Sangjun Lee. Email: sangjun@ssu.ac.kr

Received: 22 June 2026; Accepted: 27 August 2026; Published: 28 September 2026

ABSTRACT: Computational Fluid Dynamics (CFD) has become the benchmark approach for analyzing hydrogen explosions because it accurately resolves transient shock-wave propagation and complex blast-wave interactions. However, high-fidelity CFD simulations remain computationally expensive for repeated safety evaluation and large-scale parametric studies. To address this limitation, this study proposes a deep learning-based spatiotemporal surrogate framework for reconstructing transient three-dimensional (3D) hydrogen explosion overpressure fields. High-resolution CFD datasets were generated using the OpenFOAM-based `radXiFoam` solver by systematically varying blast-wall height and setback distance, producing approximately 20.4 million spatiotemporal pressure samples from 1859 monitoring locations. Three representative sequential deep learning architectures, namely Long Short-Term Memory (LSTM), Transformer, and Temporal Convolutional Network (TCN), were comparatively evaluated using an identical training and evaluation protocol. Among the investigated models, TCN achieved the highest reconstruction accuracy for an unseen interpolation test configuration, yielding a Root Mean Square Error (RMSE) of 0.001113 and a coefficient of determination (R^2) of 0.9778. The proposed framework successfully reconstructed the spatiotemporal evolution of hydrogen explosion overpressure fields, including blast-wave propagation, reflection, diffraction, and attenuation, while substantially reducing computational cost compared with conventional CFD simulations. Overall, the proposed surrogate framework provides a computationally efficient surrogate modeling approach for transient three-dimensional overpressure field reconstruction, supporting hydrogen explosion hazard assessment and protective barrier evaluation.

KEYWORDS: Hydrogen explosion; surrogate modeling; temporal convolutional network; spatiotemporal overpressure reconstruction; computational fluid dynamics; deep learning

1 Introduction

The rapid expansion of the hydrogen economy has accelerated the deployment of hydrogen infrastructure, including refueling stations, storage facilities, and transportation networks [1,2]. Although hydrogen is a promising clean energy carrier, its low ignition energy, wide flammability range, and rapid flame propagation characteristics present significant safety challenges [3,4]. In accidental leakage scenarios, hydrogen vapor cloud explosions can generate highly transient overpressure fields, posing severe structural threats in densely populated environments [5,6]. Evaluating explosion hazards and improving protective structures are therefore essential for safe hydrogen deployment. Because their effectiveness depends strongly on blast-wall height (H) and setback distance (D), accurate prediction of transient three-dimensional (3D) overpressure fields is essential for protective barrier design and quantitative safety assessment.

Computational Fluid Dynamics (CFD) is the standard tool for analyzing hydrogen explosions because it can resolve complex physical processes such as flame acceleration, turbulence–combustion interaction, shock-wave propagation, and wave reflection and diffraction under realistic geometrical conditions [7–11]. Numerous CFD studies have investigated hydrogen dispersion, explosion behavior, and the performance of protective barriers in hydrogen facilities [12]. However, resolving rapidly evolving shock fronts and steep pressure gradients requires fine spatial and temporal discretization, making high-fidelity simulations computationally expensive. Depending on the computational domain and mesh resolution, a single simulation may require several hours or even days to complete [7,9]. This computational burden limits the practical use of CFD for repeated design evaluation, parametric studies, and uncertainty quantification, motivating the development of computationally efficient surrogate models [13].

Deep learning-based surrogate models have recently attracted considerable attention as efficient alternatives to high-fidelity numerical simulations [13–15]. Prior studies have achieved high accuracy in predicting scalar metrics such as peak overpressure, impulse, safety distances, gas concentrations, and point-wise pressure histories [16–19]. Recent work has also explored sequential deep learning architectures, temporal convolutional networks, and graph neural networks for surrogate modeling and prediction of complex physical phenomena, including hydrogen safety applications [20–26]. Nevertheless, most existing approaches remain focused on scalar quantities or point-wise predictions. As a result, they cannot reconstruct the continuous spatiotemporal evolution of overpressure fields governed by wave propagation, reflection, diffraction, and attenuation. Since these physical processes directly influence blast-wall performance, point-wise predictions alone provide only limited support for field-level safety assessment.

Reconstructing transient three-dimensional (3D) overpressure fields is considerably more challenging than predicting scalar engineering quantities because a surrogate model must simultaneously represent spatial correlations, rapid temporal variations, and sharp pressure discontinuities. Although deep learning has advanced rapidly in recent years, surrogate models capable of reconstructing transient 3D hydrogen explosion overpressure fields from CFD data remain limited. In addition, the relative performance of representative sequential deep learning architectures for this problem has not been comprehensively evaluated using a consistent dataset and evaluation protocol. This study presents a deep learning-based spatiotemporal surrogate framework for reconstructing transient 3D hydrogen explosion overpressure fields. A standardized CFD dataset was generated using the OpenFOAM-based `radXiFoam` solver [27] across systematically varied blast-wall configurations, yielding approximately 20.4 million spatiotemporal pressure samples collected at 1859 monitoring locations. Long Short-Term Memory (LSTM), Transformer, and Temporal Convolutional Network (TCN) models [23–26] were evaluated using the same training procedure and an unseen interpolation test case within the design space. Unlike previous surrogate models that focus primarily on scalar responses or point-wise pressure predictions, the proposed framework reconstructs transient three-dimensional overpressure fields. It provides a surrogate modeling approach for hydrogen explosion hazard assessment and protective barrier evaluation.

2 Related Work

This section reviews the foundations of the proposed framework in three parts: (i) CFD-based hydrogen explosion analysis and its computational limitations (Section 2.1); (ii) deep learning surrogate models in hydrogen safety and the limitations of scalar prediction (Section 2.2); and (iii) sequence-learning architectures for transient explosion modeling (Section 2.3). Together, these discussions highlight the persistent research gap in transient three-dimensional (3D) overpressure field reconstruction.

2.1 CFD-Based Hydrogen Explosion Analysis

Experimental investigation of hydrogen explosions is inherently challenging because full-scale explosion tests are expensive, difficult to reproduce, and involve considerable safety risks. Consequently, Computational Fluid Dynamics (CFD) has become one of the primary tools for hydrogen explosion analysis, providing detailed predictions of transient combustion and blast-wave phenomena under realistic engineering conditions [4,7,11]. Unlike empirical correlations or simplified analytical models, CFD directly solves the governing equations of mass, momentum, energy, and species transport, enabling detailed simulation of hydrogen dispersion, flame acceleration, turbulence–combustion interactions, shock-wave propagation, and transient overpressure evolution with high spatial and temporal resolution [4].

The capability of CFD for hydrogen explosion analysis has been demonstrated in numerous studies. Middha et al. [7] investigated hydrogen leak dispersion and explosion behavior using CFD simulations and reproduced transient explosion characteristics with good agreement. Both et al. [8] and Xie et al. [10] showed that reliable prediction depends strongly on appropriate turbulence modeling and numerical resolution, while Machniewski and Molga [9] demonstrated that CFD accurately captures blast-wave propagation, reflection, and diffraction in partially confined hydrogen explosions. Beyond fundamental explosion analysis, CFD has also been applied to practical hydrogen infrastructure safety studies. Su et al. [12] investigated hydrogen-enriched natural gas leakage and dispersion in buried pipelines under various operating conditions. Kang et al. [17] constructed a CFD database for hydrogen refueling stations equipped with protective barriers and demonstrated that CFD-generated datasets can support data-driven safety assessment. Kang et al. [28] evaluated blast-wall performance using OpenFOAM simulations validated against hydrogen explosion experiments, while Kang et al. [29] employed the OpenFOAM-based `radXiFoam` solver to investigate vapor cloud explosions in hydrogen refueling stations and analyzed the influence of blast-wall geometry on shock-wave reflection, diffraction, and overpressure attenuation. Since the `radXiFoam` solver adopted in the present study has been validated against experimental hydrogen explosion measurements in these previous studies [28,29], it provides reliable high-fidelity CFD data for surrogate model development.

Despite its predictive capability, high-fidelity CFD simulations remain computationally demanding. Accurate prediction of hydrogen explosion dynamics requires fine spatial discretization and small time steps to resolve steep pressure gradients, flame acceleration, shock-wave propagation, and wave–structure interactions [8,9]. Consequently, a single three-dimensional simulation may require several hours or even days of computation depending on the computational domain and mesh resolution [7,9]. These computational demands limit the practical use of CFD for repeated design evaluation, large-scale parametric studies, and rapid engineering assessment, creating the need for computationally efficient surrogate models.

2.2 Deep Learning-Based Surrogate Modeling for Hydrogen Explosion Prediction

Building on these high-fidelity CFD datasets, deep-learning surrogate models have been developed to approximate high-fidelity CFD solutions without repeatedly solving the governing equations of mass, momentum, energy, and species transport [13–15]. Instead, surrogate models learn the nonlinear mapping between simulation inputs and outputs from spatiotemporal data and provide predictions at a small fraction of the computational cost of CFD. This computational efficiency makes surrogate models suitable for repeated parametric evaluation, uncertainty quantification, and rapid engineering assessment while maintaining agreement with high-fidelity numerical simulations.

Early applications of surrogate modeling in hydrogen safety primarily focused on predicting scalar safety metrics or localized hazard indicators rather than reconstructing transient overpressure fields. Hu et al. [16] combined CFD-generated datasets with an artificial neural network (ANN) to predict accidental hydrogen-air explosion loads. Kang et al. [17] developed machine learning models for estimating safety distances and evaluating protective barrier effectiveness in hydrogen refueling stations, while Min [18] employed multi-layer perceptrons (MLPs) to estimate peak overpressure around hydrogen storage vessels under different blast-wall configurations. Yang et al. [19] proposed a deep learning framework for identifying hydrogen leakage locations and leakage intensity for pre-ignition safety monitoring. Although these studies demonstrated the applicability of machine learning to hydrogen safety problems, their prediction targets remained limited to peak values, safety distances, leakage conditions, or other localized variables. By contrast, reconstructing transient 3D overpressure fields requires the model to learn both the spatial distribution and temporal evolution of blast-wave propagation throughout the computational domain.

Sequence-learning architectures have therefore attracted increasing attention for transient engineering problems because they explicitly model temporal dependencies in nonlinear dynamic systems. Liu et al. [20] proposed an SSA-LSTM-Multi-Head Attention framework for predicting coal-dust explosion pressure histories, demonstrating the capability of recurrent neural networks combined with attention mechanisms, although the prediction remained limited to point-wise pressure histories. Li et al. [21] introduced a probabilistic graph neural network (PGNN) for rapid hydrogen explosion prediction in hydrogen production plants, where graph representations captured interactions among monitoring points but remained confined to discrete graph nodes. Temporal Convolutional Networks (TCNs) have also been applied to nonlinear temporal prediction because dilated causal convolutions efficiently capture both short- and long-range temporal dependencies while preserving temporal causality [23,24]. Li et al. [22] applied TCN to nonlinear gas concentration forecasting, and Tofigh et al. [24] demonstrated the applicability of temporal convolution-based models to nonlinear transient engineering responses. As summarized in Table 1, existing surrogate models have primarily focused on scalar prediction, localized variables, or discrete spatial representations. The reconstruction of transient 3D hydrogen explosion overpressure fields has received comparatively little attention, indicating the need for surrogate models capable of accurately recovering the spatial and temporal evolution of explosion overpressure fields.

Table 1: Comparative summary of data-driven surrogate frameworks for transient engineering and hydrogen safety systems.

Reference	Data	Model	Target	Temporal	Limitation
Hu et al. [16]	CFD	ANN	Explosion load	No	Scalar response only
Kang et al. [17]	CFD	MLP	Safety distance	No	Scalar response only
Min [18]	CFD	MLP	Peak overpressure	No	No transient prediction
Yang et al. [19]	Exp./CFD	CNN	Leakage location	No	Pre-ignition only
Liu et al. [20]	Experimental	SSA-LSTM	Explosion pressure	Yes	Point-wise prediction
Li et al. [21]	CFD	PGNN	Explosion propagation	Yes	Discrete graph nodes
Li et al. [22]	Sensor data	TCN	Gas concentration	Yes	Different physical domain

2.3 Sequential Architectures and Research Scope

Transient 3D hydrogen explosion overpressure fields involve abrupt pressure discontinuities, localized shock fronts, wave reflection, diffraction, and rapid pressure attenuation occurring over very short time scales. Reconstructing these transient phenomena requires a surrogate model capable of preserving temporal causality while capturing both localized transient responses and long-range temporal dependencies. These requirements are addressed differently by recurrent, attention-based, and temporal convolutional sequence-learning paradigms, making it necessary to evaluate their suitability for transient hydrogen explosion overpressure reconstruction. LSTM represents recurrent sequence modeling through gated memory structures [20,25], Transformer captures global temporal dependencies using self-attention [26], whereas Temporal Convolutional Networks (TCNs) employ dilated causal convolutions to preserve temporal causality while efficiently expanding the temporal receptive field [23,24]. A systematic comparison of these representative architectures therefore provides a basis for identifying an appropriate surrogate model for transient hydrogen explosion prediction.

Based on the above considerations, this study develops a deep learning-based spatiotemporal surrogate framework for transient 3D hydrogen explosion overpressure reconstruction. LSTM, Transformer, and TCN are trained and evaluated under an identical framework using the CFD database described in Section 3.1. The study has two objectives: (i) to compare representative recurrent, attention-based, and temporal convolutional architectures for reconstructing transient hydrogen explosion overpressure fields; and (ii) to establish a computationally efficient surrogate framework capable of reconstructing transient 3D overpressure fields with substantially lower computational cost than high-fidelity CFD simulations.

3 Proposed Spatiotemporal Surrogate Framework

This section describes the proposed framework for reconstructing transient 3D hydrogen explosion overpressure fields from high-fidelity CFD data. The framework consists of four components: (i) CFD-based numerical database construction (Section 3.1), (ii) spatiotemporal data representation (Section 3.2), (iii) sequence-learning surrogate models (Section 3.3), and (iv) training strategy and evaluation protocol (Section 3.4).

3.1 CFD-Based Numerical Database Construction

Fig. 1 presents the overall workflow of the proposed surrogate framework. The workflow consists of five sequential steps: CFD simulation, numerical database construction, surrogate model training, model evaluation using RMSE and R^2, and transient 3D overpressure field reconstruction using the best-performing surrogate model. This subsection describes Steps 1 and 2 of the workflow, covering CFD simulation and numerical database construction.

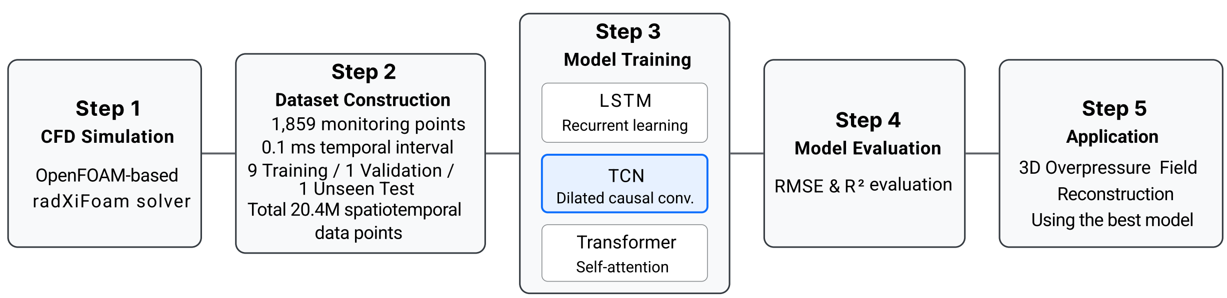

Figure 1: Overview of the proposed CFD-based deep learning surrogate framework for transient three-dimensional hydrogen explosion overpressure field reconstruction.

The CFD database was generated using the OpenFOAM-based `radXiFoam` solver [27]. As described in Section 2.1, `radXiFoam` has been validated against hydrogen explosion experiments and has been applied to hydrogen refueling station (HRS) safety analysis and blast-wall assessment [28,29]. The CFD results obtained from `radXiFoam` were used as the reference data for surrogate model training and evaluation. The computational domain, blast-wall geometry, mesh configuration, and pressure-monitoring arrangement used for database construction are shown in Fig. 2.

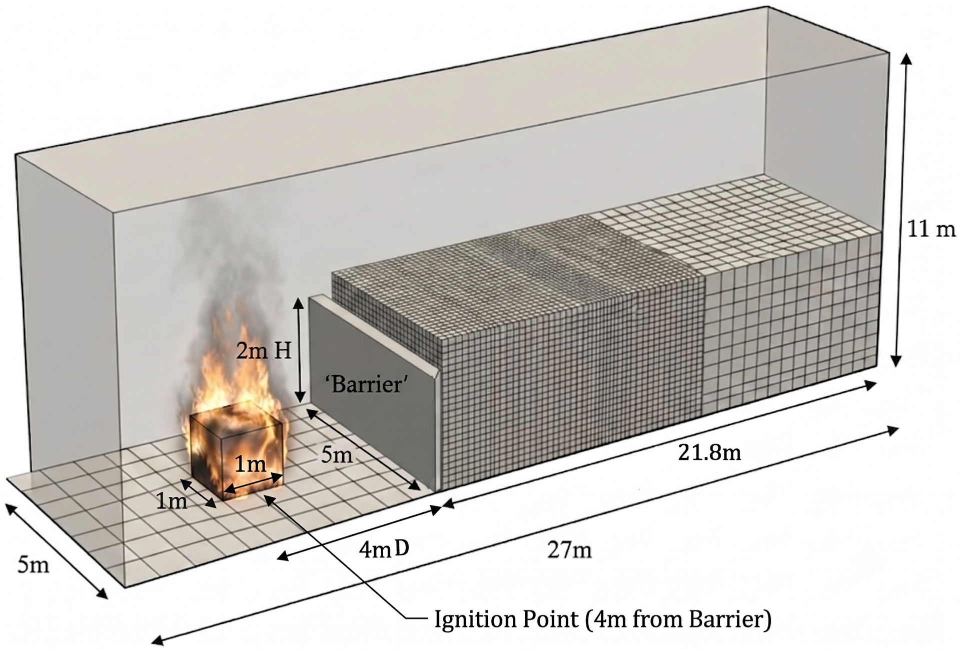

Figure 2: Representative CFD computational domain, blast-wall geometry, and mesh configuration adopted for numerical database construction. The computational domain is 27 m × 11 m × 5 m. A representative configuration with a blast-wall height of H = 2 m and a setback distance of D = 4 m is illustrated. During dataset construction, the blast-wall height (H) was varied from 2 to 4 m, while the setback distance (D) was varied from 3 to 5 m. Only transient overpressure histories in the downstream region behind the blast wall were used for surrogate-model training.

The target configuration represents an urban hydrogen refueling station equipped with a protective blast wall. Blast-wall height (H) and setback distance (D), defined as the distance between the ignition point and the blast wall, were selected as the geometric design variables because this study examines the influence of barrier geometry on explosion mitigation. Consequently, the surrogate model is intended to interpolate geometric configurations within this design space rather than predict explosion scenarios involving different physical conditions. The computational domain extends 27 m in the longitudinal direction and 11 m in the vertical direction and includes a 5 m-wide blast wall [29]. Transient pressure histories were extracted from 1859 monitoring locations distributed throughout the computational domain. To resolve the steep pressure gradients associated with hydrogen explosions, the simulations were performed with a temporal resolution of Δt = 0.1 ms. A uniform mesh size of 0.5 m was adopted in the downstream computational distance behind the blast wall, where strong blast-wave reflection and diffraction occur.

The CFD database was constructed using a full-factorial design based on blast-wall height and setback distance. The blast wall was positioned at setback distances of D = 3, 4, and 5 m from the ignition point, with corresponding blast-wall heights of H = 2, 3, and 4 m, as summarized in Table 2. Nine combinations were used for training. One intermediate configuration (H = 2.5 m, D = 4 m) was reserved for validation, whereas one unseen configuration (H = 3.5 m, D = 5 m) was reserved for testing.

The validation and test cases were selected from intermediate geometric configurations that were not included in training, thereby assessing the interpolation capability of the surrogate models within the sampled design space. The final database contains approximately 2.04×10^7 spatiotemporal pressure records collected from 1859 monitoring locations. The resulting CFD database serves as the common reference dataset for all surrogate models. Its spatiotemporal representation is described in the following subsection.

Table 2: Summary of CFD simulation scenarios used for surrogate model development based on blast-wall height (H) and setback distance (D).

Dataset	Scenario ID	H (m)	D (m)
Training	Scenario 1	2	3
Training	Scenario 2	2	4
Training	Scenario 3	2	5
Training	Scenario 4	3	3
Training	Scenario 5	3	4
Training	Scenario 6	3	5
Training	Scenario 7	4	3
Training	Scenario 8	4	4
Training	Scenario 9	4	5
Validation	Scenario A	2.5	4
Test (Unseen)	Scenario B	3.5	5

3.2 Spatiotemporal Data Representation

The CFD database described in Section 3.1 consists of transient overpressure histories recorded at 1,859 monitoring locations distributed throughout the three-dimensional (3D) computational domain under multiple blast-wall configurations. To enable efficient learning of these highly transient explosion dynamics, the raw CFD outputs were reformulated into a spatiotemporal sequence representation that simultaneously incorporates spatial coordinates, geometric design parameters, and temporal pressure histories. Specifically, the input sequence vector at time step t is defined as

$$\mathbf{X}_t = [x,\ y,\ z,\ H,\ D,\ P_{t-99},\ P_{t-98},\ \ldots,\ P_t] \tag{1}$$

where (x, y, z) denote the spatial coordinates of the monitoring locations distributed throughout the computational domain, H and D represent the blast-wall height and setback distance, respectively, and $(P_{t-99}, \ldots, P_t)$ correspond to the transient pressure history over the preceding 100 time steps. Since the temporal sampling interval of the CFD simulations was fixed at 0.1 ms, the adopted sequence length represents a physical time window of 10 ms. This hybrid representation provides the surrogate models with both geometric information and transient pressure histories, enabling them to learn localized shockwave evolution, pressure attenuation, and spatiotemporal dependencies embedded within the explosion process.

Prior to model training, all input variables were normalized to the range of $[0, 1]$ using min-max normalization to improve numerical stability and optimization convergence. The normalization procedure is expressed as

$$x_{\text{norm}} = \frac{x - x_{\min}}{x_{\max} - x_{\min}} \tag{2}$$

where $x_{\min}$ and $x_{\max}$ denote the minimum and maximum values of each variable in the numerical database, respectively. Following the preprocessing stage, the surrogate modeling problem was formulated as a one-step-ahead supervised sequence prediction task. Given the spatiotemporal input vector $\mathbf{X}_t$, the sequential deep learning models predict the overpressure at the subsequent time step according to:

$$\hat{P}_{t+1} = f(\mathbf{X}_t) \tag{3}$$

where $\hat{P}_{t+1}$ denotes the predicted overpressure at time step $t+1$, and $f(\cdot)$ represents the nonlinear mapping learned by the surrogate model. This formulation allows the models to learn the relationship between spatial location, blast-wall geometry, and local temporal evolution of explosion overpressure from high-fidelity CFD histories.

Unlike previous data-driven studies that focused primarily on scalar quantities, such as peak overpressure or localized safety metrics [16–18], the present formulation aims to reconstruct the continuous three-dimensional spatiotemporal evolution of explosion overpressure fields. Consequently, the surrogate models are required to learn the nonlinear spatiotemporal evolution of blast-wave reflection, diffraction, and attenuation throughout the entire computational domain. This spatiotemporal formulation serves as the common input representation for all sequence-learning architectures investigated in this study.

3.3 Proposed Sequential Surrogate Framework

The proposed surrogate framework aims to approximate transient 3D hydrogen explosion overpressure fields directly from CFD-generated spatiotemporal sequences using deep learning architectures specialized for temporal modeling. Within this framework, three representative sequence-learning paradigms are comparatively investigated: LSTM, Transformer, and TCN. These architectures represent three distinct temporal-learning mechanisms, namely recurrent learning, self-attention-based learning, and temporal convolution learning, respectively. This comparison aims to identify the most suitable sequence-learning paradigm for surrogate modeling within the prescribed geometric design space. To ensure a fair comparison, all models employ the identical spatiotemporal input representation described in Section 3.2 and are trained using the same CFD-generated database. Consequently, differences in predictive performance primarily reflect the temporal modeling capability of each architecture.

3.3.1 LSTM

LSTM is a recurrent neural network architecture designed to capture long-term temporal dependencies through memory cells and gating mechanisms [25]. The forget gate, which regulates the amount of historical information retained during the sequential update process, is expressed as

$$f_t = \sigma\left(W_f[h_{t-1}, x_t] + b_f\right), \tag{4}$$

where x_t denotes the input at time step t, h_{t-1} is the previous hidden state, $\sigma(\cdot)$ is the sigmoid activation function, and W_f and b_f represent trainable weight matrices and bias vectors, respectively. The LSTM model employed in this study consists of two stacked LSTM layers with 128 and 64 hidden units, respectively, followed by a fully connected layer with 64 hidden units and a single output node for one-step-ahead pressure prediction.

3.3.2 Transformer

A lightweight Transformer architecture based on Multi-Head Self-Attention (MHSA) was employed as a representative attention-based baseline for transient hydrogen explosion prediction [26]. The attention operation is formulated as

$$\text{Attention}(Q, K, V) = \text{softmax}\left(\frac{QK^T}{\sqrt{d_k}}\right)V, \tag{5}$$

where Q, K, and V denote the query, key, and value matrices, respectively, and d_k represents the dimensionality of the key vectors. The implemented Transformer architecture consists of a single Multi-Head

Self-Attention layer with four attention heads. To stabilize the training dynamics, a residual connection followed by layer normalization was applied to the attention output. The resulting features were subsequently aggregated using a global average pooling layer and processed through a fully connected layer with 64 hidden units, followed by a single output node for one-step-ahead pressure prediction. Unlike the original Transformer architecture, stacked encoder blocks and positional encoding were not incorporated in this study, as the objective was to establish a lightweight attention-based baseline under the same spatiotemporal input representation and optimization framework used for the LSTM and TCN models. This implementation provides a consistent benchmark for evaluating different temporal feature extraction mechanisms for transient hydrogen explosion prediction.

3.3.3 TCN

The TCN architecture employs dilated causal convolutions to extract temporal features while strictly preserving temporal causality [22–24]. The dilated convolution operation is given by

$$F(s) = (x *_d f)(s) = \sum_{i=0}^{k-1} f(i) x_{s-di}, \tag{6}$$

where d is the dilation factor, k is the kernel size, and $f(i)$ denotes the convolution kernel coefficient. The adopted TCN architecture consists of five temporal convolution blocks with exponentially increasing dilation factors

$$d = \{1, 2, 4, 8, 16\}, \tag{7}$$

using a fixed kernel size of $k = 3$. Each temporal convolution block contains 64 filters with residual and skip connections, which facilitate efficient feature extraction and information flow across different temporal scales. The extracted features are subsequently processed by a fully connected layer with 32 hidden units using the Rectified Linear Unit (ReLU) activation function, followed by a single output node for one-step-ahead pressure prediction. The progressively expanding receptive field enables the TCN architecture to simultaneously capture localized shockwave propagation and long-range pressure attenuation while preserving temporal causality and computational efficiency. The architectures described above were trained and evaluated under an identical optimization framework to comparatively investigate their capability for transient overpressure prediction.

3.4 Training Strategy and Evaluation Protocol

To ensure a fair and reproducible comparison of the representative sequence-learning paradigms, identical training and optimization strategies were employed for the LSTM, Transformer, and TCN architectures. All models were trained using the same CFD-generated numerical database and the uniform spatiotemporal input representation described in Sections 3.1 and 3.2. Consequently, any differences in predictive performance are expected to primarily reflect the intrinsic temporal learning characteristics of each architecture. The gradient-based optimization process was performed using the Adam optimizer because of its robust convergence characteristics for large-scale nonlinear regression problems involving spatiotemporal CFD datasets. The initial learning rate was fixed at 1×10^{-3} to achieve an appropriate balance between convergence stability and training efficiency. The objective loss function was defined as the Mean Squared Error (MSE), which is widely adopted for continuous regression problems and directly measures the discrepancy between the CFD-generated reference overpressure and the surrogate prediction, formulated as:

$$\mathrm{MSE} = \frac{1}{N}\sum_{i=1}^{N}\left(P_i - \hat{P}_i\right)^2 \tag{8}$$

where P_i and $\hat{P}_i$ denote the reference and predicted overpressure values, respectively, and N represents the total number of spatiotemporal samples used during optimization.

Considering the large-scale CFD database consisting of approximately 20.4 million spatiotemporal pressure records, a mini-batch size of 1024 was employed to achieve efficient optimization while maintaining stable gradient updates. The temporal input window length was fixed to 100 time steps, corresponding to a physical duration of 10 ms under the sampling interval of Δt = 0.1 ms. This sequence length was selected to provide sufficient temporal information for capturing shockwave propagation, localized pressure discontinuities, and subsequent attenuation behaviors associated with transient hydrogen explosions. To improve model generalization and mitigate overfitting, an early-stopping strategy was adopted with a patience parameter of five epochs. The maximum number of training epochs was set to 20, and the model weights corresponding to the minimum validation loss were automatically restored. Validation performance was monitored exclusively using Scenario A (H = 2.5 m and D = 4 m), which was excluded from parameter optimization and reserved solely for hyperparameter tuning, model selection, and early-stopping control.

Crucially, Scenario B (H = 3.5 m and D = 5 m) was completely excluded from both the training and validation procedures and was used exclusively as an independent unseen testing dataset. During testing, each prediction was generated independently from a sliding window composed of CFD reference histories. The predicted values were not recursively fed back into the input sequence. Accordingly, the present framework is formulated as a one-step-ahead supervised sequence prediction problem rather than an autoregressive multi-step forecasting task. Therefore, the final performance evaluation was conducted under an unseen geometric combination within the design space, enabling an assessment of the interpolation capability of the surrogate models.

The training hyperparameters adopted uniformly for all sequence-learning architectures are summarized in Table 3. Through this unified optimization framework and rigorously controlled evaluation protocol, the present study provides an unbiased benchmark for assessing the relative suitability of representative sequence-learning architectures and identifying the most effective surrogate framework for reconstructing transient three-dimensional (3D) hydrogen explosion overpressure fields under unseen geometric configurations.

Table 3: Training hyperparameters adopted for all surrogate models.

Hyperparameter	Value
Optimizer	Adam
Initial learning rate	1×10^{-3}
Loss function	Mean Squared Error
Batch size	1024
Maximum epochs	20
Input sequence length	100 time steps (10 ms)
Early stopping patience	5 epochs
Best weight restoration	Enabled

4 Results and Discussion

This section presents the prediction performance and spatiotemporal reconstruction capability of the proposed sequential surrogate framework for transient hydrogen explosion overpressure prediction. The comparative evaluation is organized into three complementary analyses. First, the prediction performance and computational efficiency of the LSTM, Transformer, and TCN architectures are assessed for an unseen blast-wall configuration (Section 4.1). Subsequently, the transient waveform reconstruction characteristics and prediction error distributions are comparatively analyzed to investigate the ability of each architecture to capture the highly transient characteristics of explosion overpressure evolution (Section 4.2). Finally, the spatial reconstruction capability of the selected surrogate model is evaluated through direct comparison with high-fidelity CFD reference solutions for transient 3D overpressure fields (Section 4.3).

4.1 Prediction Accuracy and Computational Efficiency

To evaluate the prediction performance of the sequential surrogate models, the LSTM, Transformer, and TCN architectures were assessed using the unseen Scenario B (H = 3.5 m and D = 5 m), which was completely excluded from both the training and validation procedures. This previously unseen blast-wall configuration provides a rigorous benchmark for assessing the capability of each architecture to reconstruct transient 3D overpressure fields. The comparative prediction accuracy and computational efficiency of the evaluated paradigms are summarized in Table 4. The reported RMSE values correspond to the normalized pressure values after min-max scaling, and the coefficient of determination (R^2) was systematically evaluated using the same normalized test dataset. The reported training times include the effect of early stopping and therefore represent the actual optimization duration required for each architecture to achieve convergence.

Table 4: Performance comparison of the evaluated deep learning architectures for the unseen Scenario B test case.

Model	RMSE	R^2	Train Time (s)
LSTM	0.001373	0.9661	157
TCN	0.001113	0.9778	114
Transformer	0.004629	0.6150	55

Among the evaluated architectures, the TCN model achieved the lowest RMSE of 0.001113 and the highest coefficient of determination (R^2 = 0.9778), indicating superior predictive performance for the unseen test scenario. The LSTM model also demonstrated competitive prediction accuracy, yielding an RMSE of 0.001373 and an R^2 value of 0.9661. In contrast, although the Transformer architecture required the shortest training time (55 s) owing to its inherently parallelizable architecture, its predictive accuracy was substantially lower, resulting in an RMSE of 0.004629 and an R^2 value of 0.6150. From the perspective of computational efficiency, the recurrent structure of the LSTM model required the longest training duration (157 s) because of sequential hidden-state propagation. In comparison, the TCN architecture achieved a favorable balance between predictive accuracy and training efficiency, yielding the lowest reconstruction error while requiring a substantially shorter training time than the LSTM model. These results suggest that computational efficiency alone does not necessarily guarantee accurate reconstruction of transient hydrogen explosion dynamics. Instead, the temporal feature extraction mechanism plays a critical role in determining prediction performance. Overall, the LSTM and TCN architectures exhibited strong predictive performance for the independent test case, whereas the Transformer model showed comparatively lower reconstruction accuracy.

4.2 Transient Waveform Reconstruction and Comparative Error Analysis

To further investigate the differences in prediction performance observed in Section 4.1, the transient waveform reconstruction characteristics of the LSTM, Transformer, and TCN architectures were comparatively analyzed using the unseen Scenario B configuration. Fig. 3 presents the reconstructed overpressure histories at a representative monitoring location together with the corresponding CFD reference solution. The selected monitoring point is located downstream of the blast wall, where strong shockwave reflection, diffraction, and attenuation phenomena are observed during transient propagation.

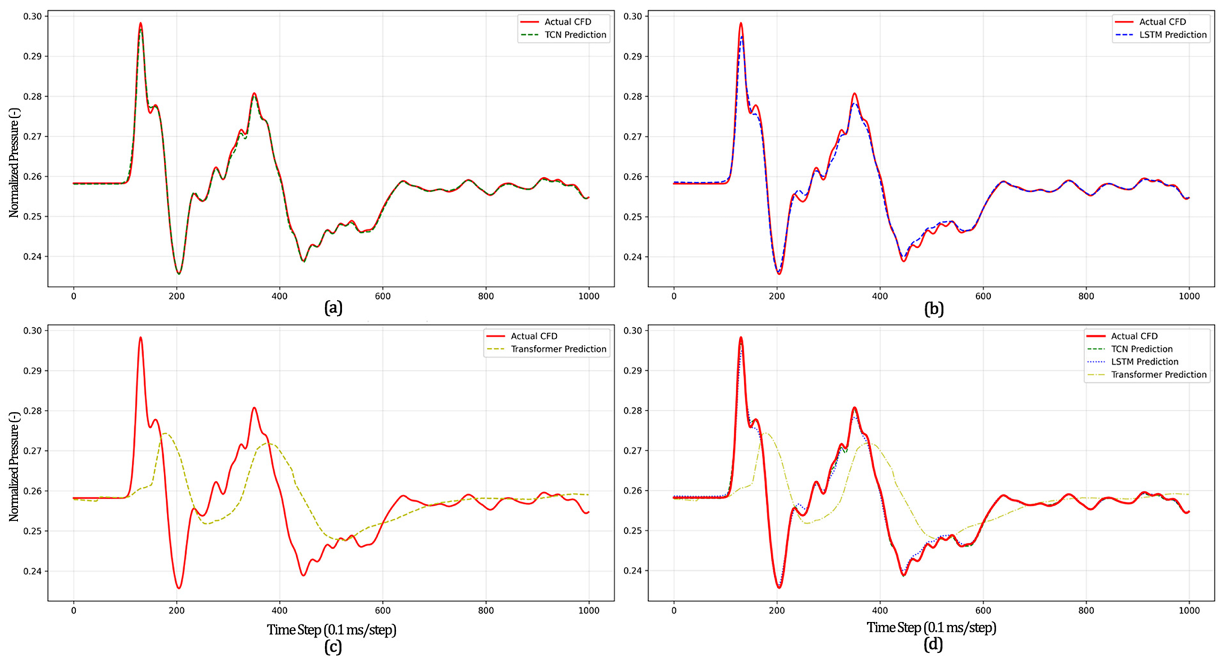

Figure 3: Comparison of reconstructed transient overpressure waveforms at the monitoring point (x = 13 m, y = 0.5 m, z = 2.5 m) for the unseen Scenario B: (**a**) TCN prediction vs. the CFD reference, (**b**) LSTM prediction vs. the CFD reference, (**c**) Transformer prediction vs. the CFD reference, and (**d**) comparison of all evaluated architectures with the CFD reference.

As illustrated in Fig. 3, all three sequence-learning architectures successfully captured the overall temporal evolution of explosion overpressure. The reconstructed waveforms accurately captured the major stages of pressure rise, peak formation, and subsequent attenuation observed in the CFD reference solution. Nevertheless, noticeable differences were observed in the prediction accuracy near abrupt pressure variations and highly transient regions associated with shockwave propagation. Among the evaluated architectures, the TCN model exhibited the closest agreement with the CFD reference throughout the entire transient sequence. In particular, the predicted pressure peaks and subsequent attenuation behavior closely followed the CFD solution, with relatively small deviations during rapid pressure transitions. The LSTM model also captured the overall temporal evolution with reasonable accuracy; however, larger deviations were observed near sharp pressure peaks and during the later stages of wave attenuation. In contrast, the Transformer model exhibited comparatively larger discrepancies from the CFD reference, particularly around regions characterized by rapid pressure variations and localized transient fluctuations.

To quantitatively evaluate these reconstruction characteristics, Fig. 4 presents the global prediction error distribution and the temporal evolution of the mean absolute error (MAE) for the three architectures.

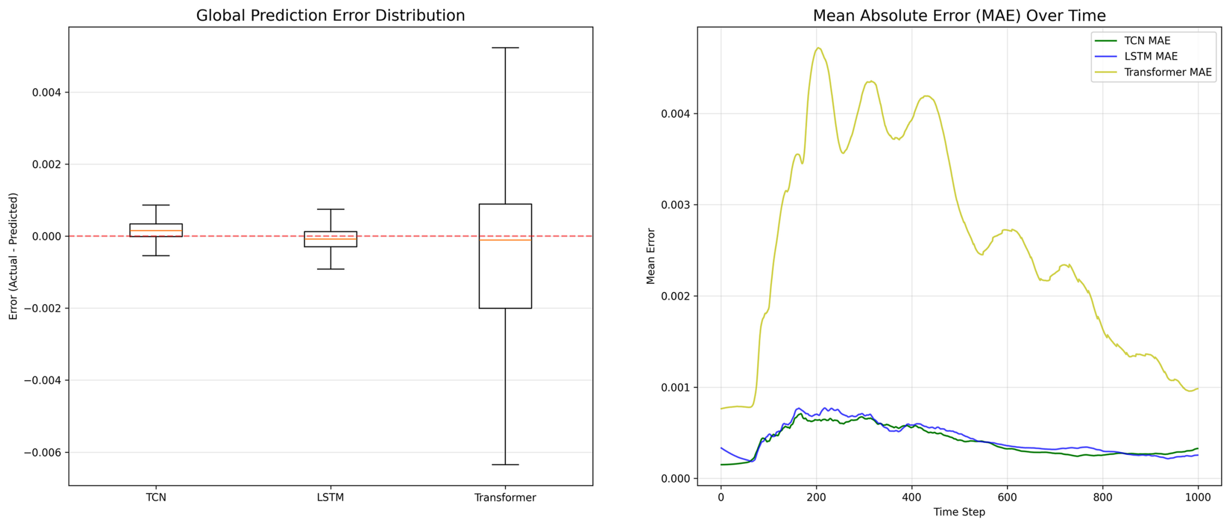

Figure 4: Comparative error analysis of sequential deep learning architectures for transient hydrogen explosion reconstruction: (**a**) global prediction error distribution based on the difference between CFD reference data and model predictions, and (**b**) temporal evolution of mean absolute error (MAE) over the transient sequence.

The prediction error distributions shown in Fig. 4a indicate that the TCN model maintained the narrowest prediction error distribution centered near zero, implying relatively stable reconstruction behavior across the entire transient sequence. The LSTM model also exhibited a concentrated error distribution but with slightly larger dispersion. In contrast, the Transformer architecture produced a broader error distribution and greater prediction variability throughout the unseen test scenario. The temporal MAE profiles presented in Fig. 4b highlight the differences in reconstruction accuracy among the evaluated architectures. The TCN model consistently maintained lower prediction errors throughout most of the transient sequence, particularly during periods of rapid pressure variation. The LSTM architecture achieved comparable performance during the early transient stages; however, its prediction errors gradually increased during later stages of the sequence. Meanwhile, the Transformer model exhibited larger MAE values over most of the temporal range, indicating comparatively lower reconstruction accuracy under highly transient explosion conditions.

Overall, the waveform reconstruction and error analyses reveal distinct reconstruction characteristics among the evaluated sequence-learning architectures. Although all three models reproduced the overall trend of transient overpressure evolution, differences were observed in their ability to capture rapid pressure variations and maintain prediction stability throughout the transient sequence. The TCN consistently showed the closest agreement with the CFD reference, which is reflected in its higher prediction accuracy reported in Section 4.1. This superior performance is considered to be associated with its dilated causal convolution architecture. By progressively expanding the receptive field while preserving local temporal information, the TCN effectively captures both rapid pressure variations and longer-term temporal evolution without relying on recurrent state updates. In contrast, the LSTM propagates information sequentially through recurrent memory, which may reduce its ability to follow abrupt pressure changes, while the Transformer architecture adopted in this study places greater emphasis on global temporal relationships than on localized transient features. Based on these comparative results, the TCN was selected for further evaluation. The following section further evaluates the selected TCN through direct comparisons between the reconstructed and CFD-generated transient 3D overpressure fields.

4.3 Spatial Overpressure Field Reconstruction

Based on the comparative evaluations presented in Sections 4.1 and 4.2, the TCN architecture was selected for further investigation of spatial reconstruction performance. To assess its ability to reproduce the spatial evolution of explosion-induced pressure waves, the transient 3D overpressure fields reconstructed by the TCN-based surrogate model were directly compared with the high-fidelity CFD reference solutions under the unseen Scenario B (H = 3.5 m and D = 5 m). The CFD reference fields were generated using the radXiFoam solver [27], which served as the high-fidelity numerical benchmark throughout this study. Fig. 5 presents the transient overpressure distributions obtained from the CFD simulations and the corresponding fields reconstructed by the TCN-based surrogate model at three representative propagation times. The selected snapshots correspond to the early shockwave propagation stage (t = 0.0070 s), the intermediate diffraction stage (t = 0.0085 s), and the later attenuation stage (t = 0.0100 s), thereby illustrating the evolution of blast-wave dynamics behind the protective blast wall.

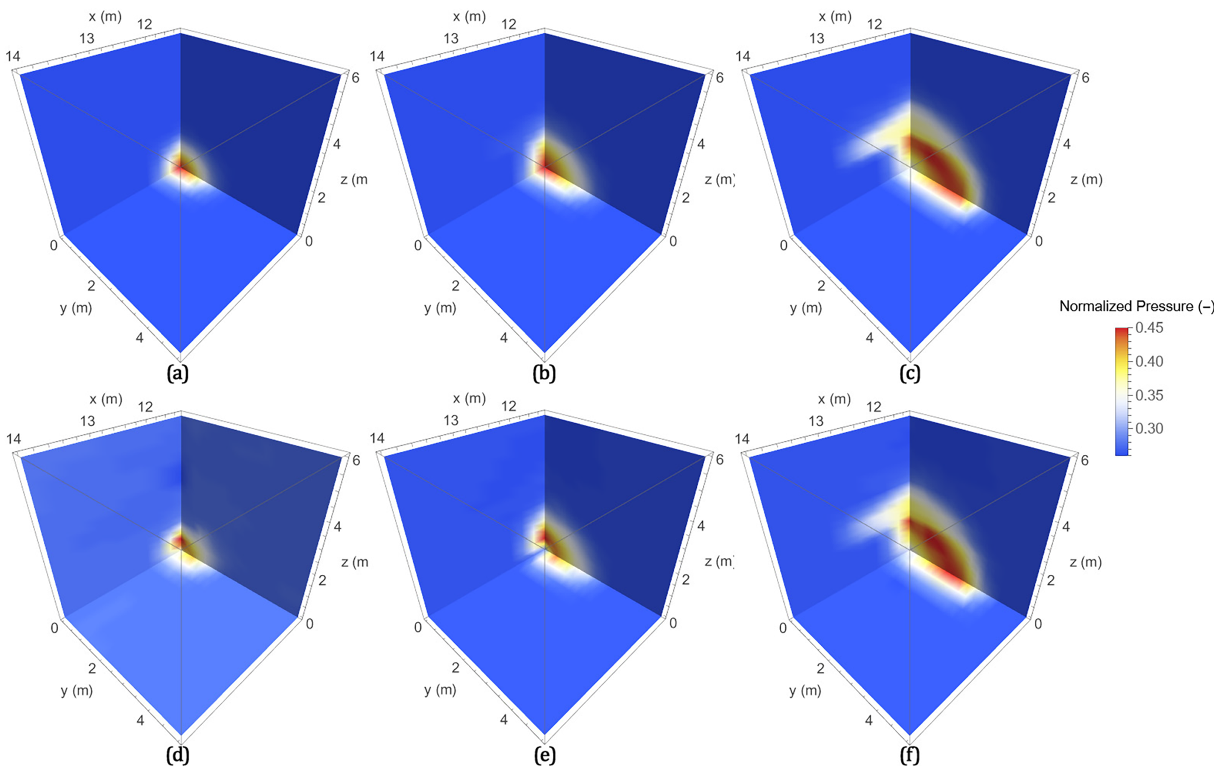

Figure 5: Comparison of transient three-dimensional overpressure fields between the CFD reference solution and the TCN-based surrogate model under the unseen Scenario B: (**a**) CFD reference at t = 0.0070 s, (**b**) CFD reference at t = 0.0085 s, (**c**) CFD reference at t = 0.0100 s, (**d**) TCN prediction at t = 0.0070 s, (**e**) TCN prediction at t = 0.0085 s, and (**f**) TCN prediction at t = 0.0100 s. The color bar represents the normalized pressure ($P/P_{\max}$).

As illustrated in Fig. 5, the TCN-based surrogate model successfully reproduced the overall spatiotemporal evolution of explosion-induced pressure waves throughout the downstream region behind the blast wall. The predicted pressure distributions exhibited close agreement with the CFD reference solutions in terms of shock-front location, pressure-wave morphology, and overall propagation behavior across all representative time instances. In particular, the locations and spatial morphology of the propagating shock fronts were accurately reconstructed during the early propagation stage (t = 0.0070 s), where strong diffraction effects occur immediately downstream of the barrier. As the transient wave propagated further downstream

(t = 0.0085 s and t = 0.0100 s), the reconstructed fields continued to preserve the major spatial features observed in the CFD simulations, including the gradual attenuation of overpressure, the expansion of the pressure-wave front, and the asymmetric propagation patterns induced by blast-wall interactions. Moreover, the TCN-based surrogate model effectively captured the reflected and diffracted wave structures behind the protective barrier while preserving the overall propagation patterns observed in the CFD simulations.

These observations indicate that the surrogate model captured the global spatiotemporal characteristics of explosion-induced overpressure propagation rather than merely approximating local pressure responses at individual monitoring locations. The ability to reconstruct evolving shockwave structures and their interactions with geometric boundaries is particularly important for practical hydrogen safety applications, where spatially resolved pressure distributions are required for hazard assessment and protective barrier design. Overall, the spatial reconstruction results demonstrate that the selected surrogate framework accurately reproduces the transient three-dimensional (3D) hydrogen explosion overpressure fields under a previously unseen blast-wall configuration. Combined with the prediction and waveform reconstruction results presented in the preceding sections, these findings indicate that deep learning-based sequential surrogate modeling can effectively capture the essential spatiotemporal characteristics of explosion-induced pressure propagation while substantially reducing the computational cost associated with high-fidelity CFD simulations. Therefore, the proposed framework offers a computationally efficient surrogate methodology that complements high-fidelity CFD simulations, enabling rapid hydrogen explosion analysis, protective barrier evaluation, and quantitative safety assessment in hydrogen infrastructure applications.

5 Conclusion

This study presented a deep learning-based spatiotemporal surrogate framework for reconstructing transient three-dimensional (3D) hydrogen explosion overpressure fields from high-fidelity CFD simulations. A standardized CFD database was generated using the OpenFOAM-based `radXiFoam` solver by systematically varying blast-wall height (H) and setback distance (D), providing approximately 20.4 million spatiotemporal pressure samples collected from 1859 monitoring locations. Using this dataset, three representative sequential deep learning architectures—Long Short-Term Memory (LSTM), Transformer, and Temporal Convolutional Network (TCN)—were evaluated under an identical training protocol and testing framework.

The comparative evaluation showed that the TCN model achieved the highest reconstruction accuracy for an unseen interpolation test case within the sampled design space, yielding an R^2 value of 0.9778 and an RMSE of 0.001113. The reconstructed overpressure fields reproduced the major characteristics of transient blast-wave propagation, reflection, diffraction, and attenuation behind protective barriers while reducing computational cost by several orders of magnitude compared with the corresponding high-fidelity CFD simulations. These results demonstrate that deep learning-based surrogate modeling can provide an efficient alternative for reconstructing transient three-dimensional hydrogen explosion overpressure fields while preserving the principal characteristics of the corresponding CFD solutions. In addition, the comparative results provide guidance for selecting appropriate sequential deep learning architectures for transient hydrogen explosion overpressure field reconstruction and establish a useful basis for future surrogate model development.

Several limitations should be acknowledged. The CFD database was generated under fixed hydrogen-air mixture and environmental conditions while varying only blast-wall height (H) and setback distance (D). Other factors that may influence explosion behavior, including hydrogen concentration, ignition location, ambient wind, and multiple obstacle configurations, were not considered in the present dataset. In addition, the proposed framework was evaluated only for interpolation within the sampled design space

($H \in [2, 4]$ m and $D \in [3, 5]$ m). Its applicability to extrapolation scenarios outside these parameter ranges remains to be investigated. Furthermore, although the CFD database was constructed using the OpenFOAM-based `radXiFoam` solver, which has been validated against hydrogen explosion experiments in previous studies, the proposed surrogate framework itself has not yet been validated against independent experimental measurements under the conditions considered in this study. Finally, the current surrogate model is entirely data-driven and does not explicitly enforce physical conservation laws or thermodynamic constraints.

Future work will therefore include experimental validation of the proposed surrogate framework using hydrogen explosion measurements while extending the CFD database to encompass a broader range of operating conditions and more complex geometrical configurations. Physics-informed learning approaches, such as Physics-Informed Neural Networks (PINNs), and advanced spatiotemporal architectures, including Graph Neural Networks (GNNs), Convolutional Long Short-Term Memory (ConvLSTM), the Fourier Neural Operator (FNO), and DeepONet, will be investigated to improve the physical consistency and generalization capability of the surrogate model. Model interpretability will also be investigated using feature attribution and visualization techniques to better understand the influence of input variables on surrogate predictions for practical hydrogen safety assessment.

Acknowledgement: Not applicable.

Funding Statement: This work was supported by Innovative Human Resource Development for Local Intellectualization Program through the Institute of Information & Communications Technology Planning & Evaluation (IITP) grant funded by the Korea government (MSIT) (IITP-2026-RS-2022-00156360).

Author Contributions: The authors confirm their contributions to the paper as follows: Jiwon Hwang: Conceptualization, Methodology, Software, Validation, Formal Analysis, Investigation, Data Curation, Writing—Original Draft Preparation, Writing—Review and Editing, Visualization. Sangjun Lee: Supervision, Writing—Review and Editing, Project Administration, Funding Acquisition. All authors reviewed and approved the final version of the manuscript.

Availability of Data and Materials: The datasets generated and analyzed during the current study were produced using the radXiFoam CFD solver. The data are available from the corresponding author upon reasonable request.

Ethics Approval: Not applicable.

Conflicts of Interest: The authors declare no conflicts of interest.

Abbreviations

ANN	Artificial Neural Network
CFD	Computational Fluid Dynamics
CNN	Convolutional Neural Network
HRS	Hydrogen Refueling Station
LSTM	Long Short-Term Memory
MAE	Mean Absolute Error
MHSA	Multi-Head Self-Attention
MLP	Multi-Layer Perceptron
MSE	Mean Squared Error
OpenFOAM	Open-source Field Operation and Manipulation (official expansion of the software name)
PGNN	Probabilistic Graph Neural Network
ReLU	Rectified Linear Unit
RMSE	Root Mean Square Error
SSA	Sparrow Search Algorithm
TCN	Temporal Convolutional Network

References

1. International Energy Agency. Global hydrogen review 2023. Paris, France: International Energy Agency; 2023.
2. Hydrogen Council; McKinsey & Company. Global Hydrogen Flows: Hydrogen Trade as a Key Enabler for Efficient Decarbonization; Brussels, Belgium: Hydrogen Council; 2022 [cited 2026 Aug 20]. Available from: https://hydrogencouncil.com/en/global-hydrogen-flows/.
3. National Fire Protection Association. NFPA 2: Hydrogen Technologies Code; Quincy, MA, USA: NFPA; 2023 [cited 2026 Aug 20]. Available from: https://link.nfpa.org/all-publications/2/2023/.
4. Molkov V. Fundamentals of hydrogen safety engineering I. London, UK: Bookboon; 2012.
5. Lea CJ, Ledin HS. A review of the state-of-the-art in gas explosion modelling. [cited 2026 Jul 31]. Available from: https://www.fabig.com/external-publications/hse-hsl200202/.
6. LaChance J, Houf W, Middleton B, Fluer L. Analyses to support development of risk-informed separation distances for hydrogen codes and standards. Albuquerque, NM, USA: Sandia National Laboratories; 2009.
7. Middha P, Hansen OR, Grune J, Kotchourko A. CFD calculations of gas leak dispersion and subsequent gas explosions: validation against ignited impinging hydrogen jet experiments. J Hazard Mater. 2010;179(1–3):84–94. doi:10.1016/j.jhazmat.2010.02.061.
8. Both AL, Atanga G, Hisken H. CFD modelling of gas explosions: optimising sub-grid model parameters. J Loss Prev Process Ind. 2019;60(1847):159–73. doi:10.1016/j.jlp.2019.04.008.
9. Machniewski P, Molga E. CFD analysis of large-scale hydrogen detonation and blast wave overpressure in partially confined spaces. Process Saf Environ Prot. 2022;158(1–3):537–46. doi:10.1016/j.psep.2021.12.032.
10. Xie H, Makarov D, Kashkarov S, Molkov V. CFD simulations of hydrogen tank fuelling: sensitivity to turbulence model and grid resolution. Hydrogen. 2023;4(4):1001–21. doi:10.3390/hydrogen4040058.
11. Gamezo VN, Ogawa T, Oran ES. Numerical simulations of flame propagation and DDT in obstructed channels filled with hydrogen–air mixture. Proc Combust Inst. 2007;31(2):2463–71. doi:10.1016/j.proci.2006.07.220.
12. Su Y, Li J, Yu B, Zhao Y, Han D, Sun D. Modeling of hydrogen blending on the leakage and diffusion of urban buried hydrogen-enriched natural gas pipeline. Comput Model Eng Sci. 2023;136(2):1315–37. doi:10.32604/cmes.2023.0260353.
13. Brunton SL, Noack BR, Koumoutsakos P. Machine learning for fluid mechanics. Annu Rev Fluid Mech. 2020;52(1):477–508. doi:10.1146/annurev-fluid-010719-060214.
14. Pathak J, Hunt B, Girvan M, Lu Z, Ott E. Model-free prediction of large spatiotemporally chaotic systems from data: a reservoir computing approach. Phys Rev Lett. 2018;120(2):024102. doi:10.1103/PhysRevLett.120.024102.
15. Karniadakis GE, Kevrekidis IG, Lu L, Perdikaris P, Wang S, Yang L. Physics-informed machine learning. Nat Rev Phys. 2021;3(6):422–40. doi:10.1038/s42254-021-00314-5.
16. Hu Q, Zhang X, Li Q, Hao H, Coffey C, Mitchell-Corbett F. Prediction and interpretability of accidental explosion loads from hydrogen-air mixtures using CFD and artificial neural network method. Int J Hydrogen Energy. 2024;66(6):135–47. doi:10.1016/j.ijhydene.2024.03.299.
17. Kang HS, Hwang JW, Yu CH. A database extension for a safety evaluation of a hydrogen refueling station with a barrier using a CFD analysis and a machine learning method. Processes. 2023;11(10):3025. doi:10.3390/pr11103025.
18. Min H. Prediction of hydrogen storage vessel explosion with blast wall using machine learning. Int J Comput Sci Mob Comput. 2024;13(7):12–22. doi:10.47760/ijcsmc.2024.v13i07.002.
19. Yang G, Kong D, He X, Yu X. Prediction of hydrogen leakage location and intensity in hydrogen refueling stations based on deep learning. Int J Hydrogen Energy. 2024;68(8):209–20. doi:10.1016/j.ijhydene.2024.04.234.
20. Liu Y, Li W, Wang H, Du T. SSA-LSTM-multi-head attention modelling approach for prediction of coal dust maximum explosion pressure based on the synergistic effect of particle size and concentration. Comput Model Eng Sci. 2025;143(2):2261–86. doi:10.32604/cmes.2025.064179.
21. Li J, Li J, Xie Z, Shi J, Li Y, Chang Y, et al. Probabilistic graph neural network-based real-time hydrogen gas explosion prediction from hydrogen production plants. Safety Emerg Sci. 2025;1(2):9590012. doi:10.26599/SES.2025.9590012.
22. Li S, Zhang S, Zhang C, Liang L, Zhang X. Temporal convolutional network for gas concentration prediction based on weighted loss and channel coupling attention. IEEE Sens J. 2025;25(6):9802–16. doi:10.1109/JSEN.2025.3529930.

23. Bai S, Kolter JZ, Koltun V. An empirical evaluation of generic convolutional and recurrent networks for sequence modeling. arXiv:1803.01271. 2018. doi:10.48550/arXiv.1803.01271.
24. Tofigh M, Kharazmi A, Smith DJ, Koch CR, Shahbakhti M. Temporal dilated convolution and nonlinear autoregressive network for predicting solid oxide fuel cell performance. Eng Appl Artif Intell. 2024;136(1):108994. doi:10.1016/j.engappai.2024.108994.
25. Hochreiter S, Schmidhuber J. Long short-term memory. Neural Comput. 1997;9(8):1735–80. doi:10.1162/neco.1997.9.8.1735.
26. Vaswani A, Shazeer N, Parmar N, Uszkoreit J, Jones L, Gomez AN, et al. Attention is all you need. In: Proceedings of the 31st International Conference on Neural Information Processing Systems; 2017 Dec 4–7; Long Beach, CA, USA. p. 5998–6008.
27. ksm0226. radXiFoam: OpenFOAM CFD solver for flamelet progress variable combustion model with radiation heat transfer. GitHub repository. [cited 2026 Mar 6]. Available from: https://github.com/ksm0226/radXiFoam.
28. Kang HS, Kim S-M, Kim J. Safety issues of a hydrogen refueling station and a prediction for an overpressure reduction by a barrier using OpenFOAM software for an SRI explosion test in an open space. Energies. 2022;15(20):7556. doi:10.3390/en15207556.
29. Kang HS, Choi KS, Lee HW, Yu CH. CFD analysis of the effects of a barrier in a hydrogen refueling station mock-up facility during a vapor cloud explosion using the radXiFoam v2.0 code. Processes. 2024;12(10):2173. doi:10.3390/pr12102173.